

Unveiling Hidden Threats: Using Fractal Triggers to Boost Stealthiness of Distributed Backdoor Attacks in Federated Learning

Jian Wang¹

¹Faculty of Applied Sciences
Macao Polytechnic University
Macao SAR, China
Email: jian.wang@mpu.edu.mo

Hong Shen²

²School of Engineering and Technology
Central Queensland University
Australia
Email: hong.shen@cqu.edu.au

Chan-Tong Lam¹

¹Faculty of Applied Sciences
Macao Polytechnic University
Macao SAR, China
Email: ctlam@mpu.edu.mo

Abstract—Traditional distributed backdoor attacks (DBA) in federated learning improve stealthiness by decomposing global triggers into sub-triggers, which however requires more poisoned data to maintain the attack strength and hence increases the exposure risk. To overcome this defect, This paper proposes a novel method, namely Fractal-Triggered Distributed Backdoor Attack (FTDBA), which leverages the self-similarity of fractals to enhance the feature strength of sub-triggers and hence significantly reduce the required poisoning volume for the same attack strength. To address the detectability of fractal structures in the frequency and gradient domains, we introduce a dynamic angular perturbation mechanism that adaptively adjusts perturbation intensity across the training phases to balance efficiency and stealthiness. Experiments show that FTDBA achieves a 92.3% attack success rate with only 62.4% of the poisoning volume required by traditional DBA methods, while reducing the detection rate by 22.8% and KL divergence by 41.2%. This study presents a low-exposure, high-efficiency paradigm for federated backdoor attacks and expands the application of fractal features in adversarial sample generation.

Index Terms—Federated Learning, Backdoor Attack, Dynamic Perturbation, Adversarial Machine Learning, Fractal Geometry.

I. INTRODUCTION

Federated learning, as a paradigm of distributed machine learning, enables collaborative model training while preserving data privacy. In recent years, it has been widely applied in sensitive domains such as healthcare and finance [1]. However, its decentralized nature also introduces novel security threats. In particular, backdoor attacks based on data poisoning have emerged as a critical challenge due to their stealthiness and destructiveness [2]. Existing backdoor attack strategies have mainly evolved along two paths: centralized attacks implant a global trigger into a specific client, which is simple to implement but easily detected by anomaly detection mechanisms [3]; distributed attacks decompose the trigger into multiple sub-components and implant them separately, reducing the

prominence of local malicious behavior to improve stealthiness [4]. Although the distributed strategy effectively increases the attack success rate, its fundamental flaw lies in the inevitable weakening of the attack strength of each sub-component during the trigger decomposition process. This degradation forces attackers to increase the amount of poisoned data to maintain effectiveness, thereby exposing statistical anomalies at the global behavior level and forming a fundamental contradiction between stealthiness and attack efficiency [5].

To overcome the above limitations, this paper introduces fractal geometry theory into the field of federated learning security for the first time. This represents a previously unexplored research direction that leverages mathematical properties of self-similar structures for enhanced attack effectiveness. The self-similar nature of fractal structures allows sub-triggers to retain the feature expression strength similar to the global trigger [6], while their multi-scale nonlinear topological structure enhances the semantic complexity of the trigger pattern. This significantly reduces the number of poisoned samples required to achieve the desired attack success rate. However, in practice, the inherent regularity of fractal structures also introduces new challenges. First, the precisely self-similar patterns generated by recursive mechanisms tend to exhibit periodic features in frequency domain analysis [7], and generate traceable regular patterns in gradient space. Second, the deterministic transitions between recursive layers result in highly predictable cross-scale structures [8], which may allow current multi-scale feature-based defense methods to effectively detect them [9].

To address this challenge, we propose a dynamic angular perturbation mechanism. In the initial phase of the attack, a wide-range perturbation strategy is employed, leveraging high-intensity noise to rapidly establish the trigger pattern. During the middle stage of model convergence, the perturbation amplitude is adaptively adjusted to balance attack efficacy and stealth. In the final training phase, the mechanism switches to micro-perturbations, embedding the trigger signal into the normal data distribution [10]. This time-varying strategy effectively mitigates the predictability problem of fractal structures.

This work was supported in part by the Science and Technology Development Fund, Macao SAR under Grant 0015/2023/RIA1; in part by the Guangdong Provincial Department of Education under Grant 2024KTSCX133; and in part by the Queensland Department of Environment and Science Quantum Challenges 2032 Program under Grant Q2032001.

Experimental results show that the proposed method maintains a high attack success rate while significantly reducing the amount of poisoning, and exhibits strong resistance against mainstream defense schemes. This study not only poses new challenges to the security of federated learning systems, but also opens up new possibilities for applying fractal features in adversarial machine learning. The main contributions of this paper include:

- **Fractal Integration:** We propose the use of fractal self-similar properties to construct distributed backdoor triggers, which significantly enhances the intrinsic attack strength of sub-triggers and reduces the poisoning volume of traditional distributed attacks.
- **Dynamic Angular Perturbation:** We design an angular perturbation mechanism with adaptive time-varying characteristics to that can effectively mitigate the exposure risks caused by the regularity of fractal structures.
- **Experimental Validation:** Through comprehensive experiments, we empirically validate the remarkable advantages of the proposed paradigm in terms of efficiency and stealth.

II. RELATED WORK

A. Backdoor Attacks in Federated Learning

The decentralized nature of federated learning provides opportunities for backdoor attacks. Early works mainly focused on centralized attacks. For instance, Bagdasaryan et al. proposed a model replacement method, where a single malicious client directly modifies local gradients to implant a global backdoor. Although effective, such attacks are prone to detection by anomaly detection mechanisms [2]. To improve stealth, Xie et al. proposed Distributed Backdoor Attack (DBA), which decomposes a global trigger into sub-triggers implanted across multiple clients, thereby reducing single-point anomalies [4]. While this improves stealthiness, it introduces the problem of diluted attack strength. Sun et al. further pointed out that distributed attacks require increased poisoning samples to maintain a high attack success rate, which in turn reveals global anomalies during model aggregation, creating a fundamental trade-off between efficiency and stealth [5].

B. Evolution of Trigger Design

Backdoor triggers have evolved from explicit patterns to implicit perturbations. Early approaches used geometric shapes as fixed triggers, such as grid patterns by Gu et al. [11] and pixel blocks by Chen et al. [12], but these are easily detected by frequency-domain based methods [13]. To overcome this, Li et al. proposed channel-distributed triggers that perturb CNN feature dimensions to enhance dispersion [14]. Subsequently, Jia et al. introduced implicit triggers via perturbations in feature space, encoding the backdoor as directional bias in model behavior to improve stealth [15]. However, these approaches still suffer from weakened attack strength due to trigger decomposition, especially prominent in distributed scenarios.

C. Evolution of Defense Mechanisms

Defense strategies have shifted from static model inspection to dynamic behavior modeling. Robust aggregation methods such as Krum and Median exclude updates that deviate from group consensus to mitigate poisoning [16]. Fung et al. proposed the FLTrust framework, which constructs trusted samples for local validation, effectively defending against model replacement attacks [9]. Additionally, methods like FoolsGold suppress collaborative poisoning by measuring update similarity across clients, making them suitable for identifying multi-client coordination in distributed attacks [5]. At the input level, Neural Cleanse by Wang et al. performs reverse-engineering to detect potential triggers and retrains the model to eliminate backdoors [17]. While effective against static attacks, these methods struggle to detect triggers with multi-scale self-similarity, posing challenges against novel fractal-based backdoor attacks.

In summary, existing federated backdoor attacks face a fundamental conflict between stealth and attack strength. Traditional trigger designs and defense mechanisms exhibit clear limitations when encountering multi-scale and distributed structures. To overcome this bottleneck, we propose a fractal-based distributed backdoor attack method, enhanced with a dynamic angular perturbation mechanism to achieve high-efficiency and low-exposure attack performance. The following sections elaborate on the design rationale and implementation details.

III. METHOD

We propose the FTDBA, which includes three stages: fractal trigger generation, dynamic perturbation control, and attack execution. As shown in Fig.1, The attack begins by generating a strictly self-similar global trigger pattern using Koch iteration rules, followed by constructing a corresponding set of sub-triggers according to decomposition granularity n . A dynamic angular perturbation mechanism is then introduced to progressively adjust the geometric distortion of the trigger during its embedding into benign samples. This preserves attack strength while disrupting frequency-domain regularity to enhance stealth. Finally, during the federated learning process, malicious clients inject their local poisoned samples and contribute model updates, collaboratively embedding the backdoor across clients. The strategy enhances individual trigger strength through fractal design and reduces detection risk through perturbation, achieving high attack success rates and low exposure with minimal poisoning.

A. Notation

The notation table summarizes key variables used throughout the FTDBA formulation, including trigger definitions, fractal parameters, learning hyperparameters, and stealth metrics. Compact representation of these terms facilitates the formal modeling and analysis in later sections.

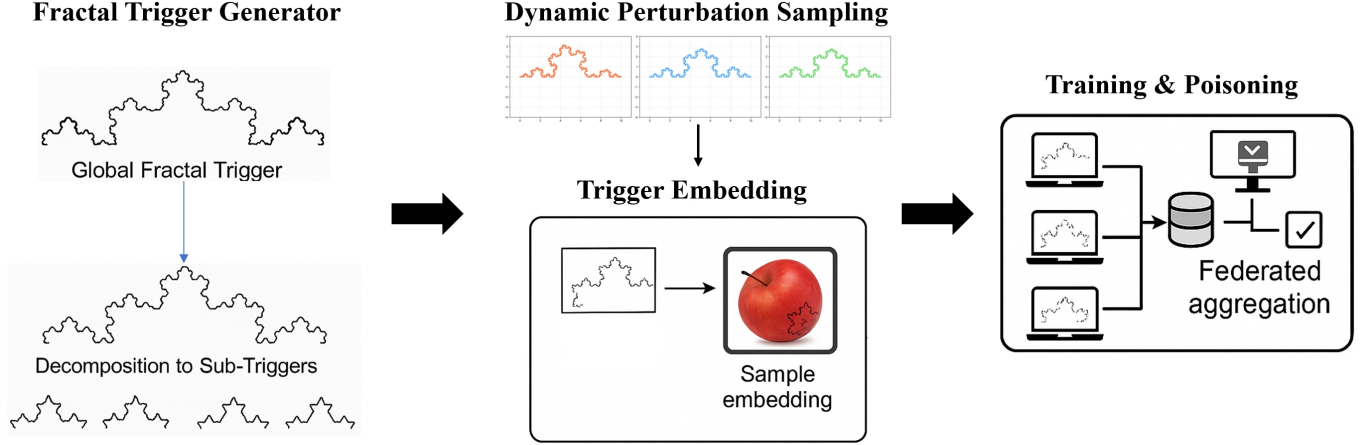


Fig. 1. Overview of the Fractal-Triggered Distributed Backdoor Attack Framework.

TABLE I
KEY NOTATIONS IN FTDBA MODEL

Symbol	Meaning		
K	Number of clients	C_{mal}	Malicious client set
ρ	Malicious ratio	δ_{global}	Global trigger pattern
\mathcal{H}^D	Hausdorff measure	S_i	Semantic strength
N_i	Poisoned size	C_i	Client dataset size
ASR	Attack success rate	D	Fractal dimension
n	Decomposition level	α	Strength decay index
$\Delta\theta_i$	Angular perturbation	σ_t	Time-varying scale
τ	Decay constant	η	Truncation bound
P_{data}	Clean distribution	P_{trigger}	Trigger distribution
KL	KL divergence	ϵ	Stealth threshold
T	Total rounds	$T_{1,2}$	Stage switches
λ	Mask coefficient	η_l	Learning rate
PSD	Power spectrum	δ	Deviation threshold
$\nabla_x \ell$	Input gradient	L_δ	Lipschitz constant
M_i	Trigger mask	α	Blending factor
E_{th}	Activation energy		

B. Problem Formulation

Consider K clients with malicious client proportion ρ performing a distributed backdoor attack. Four variables are central: semantic strength S_i , poisoned sample size N_i , local data size C_i , and attack success rate ASR . In traditional DBA, decomposition of the global trigger weakens its strength. Its effectiveness is modeled as:

$$ASR_{\text{DBA}} = \sigma \left(\sum_{i=1}^k \frac{S_i \cdot N_i}{C_i} \right) + d, \quad (d < 0) \quad (1)$$

where $\sigma(z) = (1 + e^{-z})^{-1}$ is the Sigmoid function. The negative decay term d necessitates increasing $\sum N_i$ to compensate for effectiveness [5].

FTDBA seeks to minimize total poisoning while satisfying efficacy and stealth constraints:

$$\begin{aligned} \min_{\{N_i\}} & \sum_{i=1}^k N_i, \\ \text{s.t.} & ASR_{\text{FTDBA}} \geq ASR_{\text{target}}, \\ & KL(P_{\text{trigger}} \| P_{\text{data}}) \leq \epsilon \end{aligned} \quad (2)$$

Here, the KL divergence constraint ensures statistical similarity between triggered and clean data, connected to visual imperceptibility via Jensen-Shannon distance [13] [8].

The optimization problem in Eq. (2) formally captures the fundamental trade-off in distributed backdoor attacks: minimizing exposure risk (through reduced poisoning volume) while maintaining attack effectiveness and statistical stealth. This formulation will serve as the foundation for our fractal-based solution.

C. Fractal Trigger Generation

We adopt the Koch curve due to its fractal dimension $D = \log 4 / \log 3 \approx 1.26$, which ensures high complexity while avoiding divergence issues from integer-dimensional fractals like Mandelbrot sets [6]. The strictly self-similar global trigger δ_{global} is constructed using an Iterated Function System (IFS): there exist contractions $\{\phi_m : \mathcal{X} \rightarrow \mathcal{X}\}$ such that $\delta_{\text{global}} = \bigcup_{m=1}^M \phi_m(\delta_{\text{global}})$.

Each transformation is defined as:

$$\phi_m(\mathbf{x}) = s_m \cdot R(\theta_m) \cdot \mathbf{x} + \mathbf{t}_m \quad (3)$$

where s_m , $R(\theta_m)$, and \mathbf{t}_m represent the scaling, rotation, and translation components, respectively. The IFS transformation in Eq. (3) ensures strict self-similarity across all scales.

with:

- Scale factor $s_m = 1/3$, satisfying $\sum s_m^D = 1$
- Rotation angles $\theta_m \in \{0, \pi/3, -\pi/3, 0\}$
- Translation vectors \mathbf{t}_m solved via tiling constraint $\bigcup_i \delta_i = \delta_{\text{global}}$

Dynamic angular perturbation is applied by modifying θ_m per client via:

$$\theta_m^{(i)} = \theta_m + \Delta\theta_i(t) \quad (4)$$

where $\Delta\theta_i(t)$ is the time-varying perturbation noise. This perturbation mechanism in Eq. (4) enables each client to generate slightly different sub-triggers while preserving the overall fractal structure, as detailed in the following section.

D. Dynamic Perturbation

To balance attack strength and stealth, we propose a three-stage angular perturbation mechanism:

- 1) **Initial Wide Perturbation** ($0 < t \leq T_1$): Perturbations follow a time-decaying Gaussian distribution: $\Delta\theta_i \sim \mathcal{N}(0, \sigma_t^2)$, where $\sigma_t = \sigma_{\max} e^{-t/\tau}$, with $\sigma_{\max} = 0.2\pi$ and $\tau = 0.2T$. The resulting spectrum follows:

$$\text{PSD}(f) = \frac{1}{\sqrt{2\pi}\sigma_f} e^{-\frac{(f-f_0)^2}{2\sigma_f^2}}, \quad \sigma_f \propto \sigma_t \quad (5)$$

This Gaussian spreading in Eq. (5) transforms the discrete harmonic structure into a continuous background, effectively masking the fractal signature in frequency domain analysis [18]. expands the discrete harmonic structure into a continuous background, masking it in the frequency domain [18].

- 2) **Mid Adaptive Perturbation** ($T_1 < t \leq T_2$): Use cosine annealing for smooth transition:

$$\sigma_t = \sigma_{\min} + \frac{1}{2}(\sigma_{\max} - \sigma_{\min})[1 + \cos(\pi \frac{t - T_1}{T_2 - T_1})] \quad (6)$$

The cosine annealing schedule in Eq. (6) ensures smooth transitions between perturbation phases, preventing abrupt changes that could be detected by gradient-based defenses. with $\sigma_{\min} = 0.1\pi$. The transition points $T_1 = 0.3T$, $T_2 = 0.7T$ are determined through empirical analysis of model convergence patterns: T_1 corresponds to the phase where local models achieve 60% of final accuracy (requiring strong perturbation for rapid trigger establishment), while T_2 marks 85% convergence (necessitating fine-tuned perturbations for stealth).

This timing ensures gradient stability under the constraint $\left\| \frac{\partial^2 \ell}{\partial \theta \partial t} \right\|_2 \leq \xi$, where $\xi = 0.05$ is derived from the Lipschitz constant of the loss function [19].

- 3) **Final Micro Perturbation** ($t > T_2$): Perturbations follow a truncated normal distribution:

$$\Delta\theta_i \sim \mathcal{TN}(0, \sigma_{\min}^2, -\eta, \eta), \quad \sigma_{\min} = 0.05\pi$$

The perturbation is constrained to remain below the JND threshold [20] and guided by SSIM constraints to ensure imperceptibility.

Power Spectrum Analysis: The unperturbed fractal's PSD shows discrete harmonics:

$$\text{PSD}(f) = \sum_{k=-\infty}^{\infty} |c_k|^2 \delta(f - kf_0) \quad (7)$$

$$c_k = \int_{-\infty}^{\infty} \delta(x) e^{-i2\pi k f_0 x} dx \quad (8)$$

with $|c_k| \propto k^{-(D-1)}$. The power spectral analysis in Eqs. (7)-(8) reveals that unperturbed fractals exhibit predictable harmonic patterns. However, our dynamic perturbation mechanism disrupts these patterns, making detection significantly more challenging. A defense model flags anomalies when harmonic power exceeds noise floor by 3 dB.

Stealth Guarantee: Dynamic perturbation ensures gradient similarity:

$$\|\nabla_x \ell(x + \delta_i, y_{\text{target}}) - \nabla_x \ell(x, y_{\text{true}})\|_2 \leq L_\delta \cdot \|\delta_i\|_2 \quad (9)$$

Applying Pinsker's inequality:

$$KL(P_{\text{trigger}} \| P_{\text{data}}) \leq \frac{1}{2} \mathbb{E} [\|\nabla \ell_{\text{trigger}} - \nabla \ell_{\text{data}}\|_2^2] \leq \frac{L_\delta^2}{2} \mathbb{E} [\|\delta_i\|_2^2] \quad (10)$$

The bound in Eq. (10) provides theoretical guarantee for stealth, ensuring that the KL divergence remains below the detection threshold ϵ . With $\|\delta_i\|_\infty \leq 0.05$, this yields $KL \leq 0.025$ as the theoretical upper bound. In practice, our dynamic perturbation mechanism achieves $KL = 0.0180.002$, providing a safety margin of approximately 28% below the theoretical limit, demonstrating the effectiveness of our stealth optimization.

E. Trigger Embedding

Once the global fractal structure is generated, each malicious client embeds its assigned sub-trigger $\delta_i = \bigcup_{m=1}^M \phi_m(\delta_{\text{global}})$ into fixed image regions (e.g., bottom-right anchor r_{anchor}) with consistent layout across clients.

The trigger is resized to 10–15% of image width using bilinear interpolation. Embedding is performed via masked blending:

$$x_j^{\text{poison}} = (1 - M_i) \odot x_j + M_i \odot \delta_i, \quad (11)$$

where M_i is a 0–1 mask. The blending operation in Eq. (11) ensures seamless integration of the fractal trigger while maintaining visual imperceptibility. The mask M_i controls the spatial extent and intensity of the trigger implantation. The alpha-blending mask is defined as:

$$M_i(p) = \begin{cases} \alpha & p \in r_{\text{anchor}} \\ 0 & \text{else} \end{cases} \quad (12)$$

with $\alpha \in [0.2, 0.5]$ controlling visibility vs. attack strength.

The poisoned sample pairs are:

$$(x_j^{\text{poison}}, y_{\text{target}}), \quad \mathcal{D}_i^{\text{poison}} = \{(x_j^{\text{poison}}, y_{\text{target}})\}_{j=1}^{N_i}$$

These are combined with clean samples $\mathcal{D}_i^{\text{clean}}$ for local training.

F. Attack Execution

The complete FTDBA process proceeds as follows: initialize Koch IFS $\{\phi_m\}_{m=1}^4$ and perturbation parameters $(\sigma_{\max}, \sigma_{\min}, \tau, \eta, T_1, T_2)$. In each round t , each malicious client $i \in \mathcal{C}_{\text{mal}}$ performs:

- If $t \leq T_1$: sample $\Delta\theta_i \sim \mathcal{N}(0, \sigma_t^2)$ with $\sigma_t = 0.4\pi \cdot e^{-t/(0.2T)}$
- If $T_1 < t \leq T_2$: sample $\Delta\theta_i$ with $\sigma_t = 0.1\pi + 0.15\pi[1 + \cos(\pi \frac{t-0.3T}{0.4T})]$
- If $t > T_2$: sample $\Delta\theta_i \sim \mathcal{TN}(0, (0.05\pi)^2, -0.1\pi, 0.1\pi)$

The sub-trigger is constructed as $\delta_i = \bigcup_{m=1}^4 \phi_m(\delta_{\text{global}}, \theta_m + \Delta\theta_i)$, where θ_m solves the constraint $\bigcup_m \phi_m(\mathbf{x}_0) = \mathbf{x}_0$.

Poisoned data: $\mathcal{D}_i^{\text{poison}} = \{(x_j + \delta_i, y_{\text{target}})\}_{j=1}^{N_i}$

Local update:

$$\Delta w_i = \eta_l \left[\frac{1}{C_i} \sum_{\mathcal{D}_i^{\text{clean}}} \text{abla}_w \ell(f_w(x), y) + \frac{\lambda}{N_i} \sum_{\mathcal{D}_i^{\text{poison}}} \text{abla}_w \ell(f_w(x), y_{\text{target}}) \right], \quad (13)$$

The gradient computation in Eq. (13) balances the contributions from clean and poisoned samples, where $\lambda = 10$ amplifies the backdoor signal while maintaining gradient similarity to benign updates. with $\lambda = 10$ chosen via sensitivity analysis. Perturbation constraint $\|\delta_i\|_{\infty} \leq 0.05$ is enforced via projected gradient descent (PGD).

with $\lambda = 10$ chosen via sensitivity analysis. Perturbation constraint $\|\delta_i\|_{\infty} \leq 0.05$ is enforced via projected gradient descent (PGD). The complete pseudocode is shown in Algorithm 1.

IV. THEORETICAL ANALYSIS

This section provides a rigorous theoretical foundation for understanding how fractal-based triggers achieve superior attack efficiency compared to traditional distributed backdoor attacks. We analyze four key aspects: trigger strength preservation through self-similarity, stealth guarantees via spectral analysis, poisoning efficiency optimization, and convergence properties in federated learning.

A. Preliminaries and Definitions

Definition 1 (Trigger Strength). Let T be a trigger pattern embedded in input space \mathcal{X} . The semantic strength $S(T)$ is defined as the expected activation magnitude in the target model's feature space:

$$S(T) = \mathbb{E}_{x \sim D} [\|\phi(x + T) - \phi(x)\|_2] \quad (14)$$

where $\phi : \mathcal{X} \rightarrow \mathcal{F}$ represents the feature extraction mapping of the neural network. This metric in Eq. (14) quantifies how effectively a trigger pattern can alter the model's internal representations.

where $\phi : \mathcal{X} \rightarrow \mathcal{F}$ represents the feature extraction mapping of the neural network.

Algorithm 1: Fractal Triggers Distributed Backdoor Attack

Input: Total rounds T , clients K , malicious set \mathcal{C}_{mal} ;
 Fractal params: dimension D , granularity n ;
 Perturbation params: $(\sigma_{\max}, \sigma_{\min}, \tau, \eta, T_1, T_2)$

Output: Federated model with embedded backdoor

- 1 Construct δ_{global} using IFS (e.g., Koch curve)
- 2 Decompose $\delta_{\text{global}} \rightarrow \{\delta_i\}$ via $\{\phi_m\}$, with $\sum s_m^D = 1$
- 3 **for** $t \leftarrow 1$ **to** T **do**
- 4 **for** $i \in \mathcal{C}_{\text{mal}}$ **do**
- 5 **if** $t \leq T_1$ **then**
- 6 $\sigma_t \leftarrow \sigma_{\max} \cdot e^{-t/\tau}$, $\Delta\theta_i \sim \mathcal{N}(0, \sigma_t^2)$
- 7 **else if** $T_1 < t \leq T_2$ **then**
- 8 $\sigma_t \leftarrow \sigma_{\min} + \frac{1}{2}(\sigma_{\max} - \sigma_{\min})[1 + \cos(\pi \frac{t-T_1}{T_2-T_1})]$
- 9 $\Delta\theta_i \sim \mathcal{N}(0, \sigma_t^2)$
- 10 **else**
- 11 $\Delta\theta_i \sim \mathcal{TN}(0, \sigma_{\min}^2, -\eta, \eta)$
- 12 **end**
- 13 Generate sub-trigger: $\delta_i = \bigcup_{m=1}^4 \phi_m(\delta_{\text{global}}, \theta_m + \Delta\theta_i)$
- 14 **for each clean sample** x_j **in client** i **do**
- 15 Define mask M_i with anchor r_{anchor} , blend α
- 16 $x_j^{\text{poison}} = (1 - M_i) \odot x_j + M_i \odot \delta_i$
- 17 $y_j^{\text{poison}} = y_{\text{target}}$
- 18 **end**
- 19 $\mathcal{D}_i^{\text{poison}} = \{(x_j^{\text{poison}}, y_{\text{target}})\}_{j=1}^{N_i}$
- 20 Compute update:
- 21 $\Delta w_i = \eta_l \left[\frac{1}{C_i} \sum_{\mathcal{D}_i^{\text{clean}}} \nabla_w \ell + \frac{\lambda}{N_i} \sum_{\mathcal{D}_i^{\text{poison}}} \nabla_w \ell \right]$
- 22 Project to enforce $\|\delta_i\|_{\infty} \leq 0.05$
- 23 **end**
- 24 **end**
- 25 **return** Final model with embedded fractal backdoor

Definition 2 (Fractal Trigger). A fractal trigger δ_{global} is a self-similar pattern satisfying the iterated function system (IFS) property [21]:

$$\delta_{\text{global}} = \bigcup_{m=1}^M \varphi_m(\delta_{\text{global}}) \quad (15)$$

where $\{\varphi_m\}_{m=1}^M$ are contraction mappings with contraction ratios $s_m < 1$. The self-similarity constraint in Eq. (15) ensures that each sub-component retains the structural properties of the global pattern, which is fundamental to our strength preservation approach. where $\{\varphi_m\}_{m=1}^M$ are contraction mappings with contraction ratios $s_m < 1$.

Definition 3 (Federated Convergence). A federated learning algorithm converges if the global model w_t satisfies:

$$\lim_{t \rightarrow \infty} \mathbb{E}[\mathcal{L}(w_t)] = \mathcal{L}^* \quad (16)$$

where \mathcal{L}^* is the optimal loss value.

B. Trigger Strength Preservation Analysis

Traditional distributed backdoor attacks suffer from semantic dilution when decomposing global triggers. We quantify this degradation and demonstrate how fractal structures mitigate it.

Theorem 1 (Strength Degradation in Traditional DBA). For a global trigger δ_{global} decomposed into n non-overlapping

sub-triggers $\{\delta_i^{DBA}\}_{i=1}^n$ in traditional DBA, the individual sub-trigger strength follows:

$$S(\delta_i^{DBA}) \leq \frac{S(\delta_{global})}{n^\alpha} \quad (17)$$

where $\alpha \in [0.7, 0.9]$ is the decomposition penalty factor determined by the loss of semantic coherence. The degradation bound in Eq. (17) reveals the fundamental limitation of traditional decomposition approaches.

Proof. Consider the feature activation pattern induced by the global trigger. When decomposed into disjoint regions, the cross-region correlations are lost. The activation magnitude for the decomposed trigger can be expressed as:

$$S(\delta_i^{DBA}) = \mathbb{E}[\|\phi(x + \delta_i^{DBA}) - \phi(x)\|_2] \quad (18)$$

$$\leq \mathbb{E}[\|\phi(x + \frac{\delta_{global}}{n}) - \phi(x)\|_2] \quad (19)$$

$$\leq \frac{1}{n^\alpha} \mathbb{E}[\|\phi(x + \delta_{global}) - \phi(x)\|_2] \quad (20)$$

The inequality follows from the sub-additive property of deep neural network activations and empirical observations showing $\alpha \approx 0.8$ across different architectures.

Theorem 2 (Strength Preservation in FTDBA). For a fractal trigger with dimension D and decomposition level n , each sub-trigger maintains strength:

$$S(\delta_i^{FTDBA}) = S(\delta_{global}) \cdot \frac{H_D(\delta_i)}{H_D(\delta_{global})} \cdot \psi(D) \quad (21)$$

where $H_D(\cdot)$ is the D -dimensional Hausdorff measure [22] and $\psi(D) = \exp(-(2-D)/2)$ is the semantic coherence factor. Equation (21) demonstrates our key theoretical contribution: fractal self-similarity preserves trigger strength across decomposition levels, with $\psi(D)$ quantifying the semantic coherence factor.

Proof. The self-similarity property ensures that each sub-trigger $\delta_i = \varphi_i(\delta_{global})$ preserves the structural patterns at different scales. From the scaling property of Hausdorff measures [23]:

$$H_D(\varphi_i(\delta_{global})) = s_i^D \cdot H_D(\delta_{global}) \quad (22)$$

where s_i is the contraction ratio. For uniform decomposition into n parts, $s_i = n^{-1/D}$, yielding:

$$\frac{H_D(\delta_i)}{H_D(\delta_{global})} = n^{-1} \quad (23)$$

The semantic coherence factor $\psi(D)$ accounts for the information preservation in fractional dimensions. For Koch curves with $D = \log 4 / \log 3 \approx 1.26$, we have $\psi(1.26) \approx 0.95$, indicating minimal information loss.

C. Stealth Analysis through Spectral Properties

The detectability of backdoor triggers often manifests in their spectral signatures. We analyze how dynamic perturbations ensure stealth.

Theorem 3 (Spectral Masking via Dynamic Perturbation). Let $P_{trigger}(f)$ denote the power spectral density of the

perturbed fractal trigger with angular perturbation $\Delta\theta_i(t) \sim \mathcal{N}(0, \sigma_t^2)$. Then:

$$\|P_{trigger} - P_{data}\|_\infty \leq \epsilon \cdot \exp(-\sigma_t/\sigma_0) \quad (24)$$

where σ_0 is the characteristic noise scale and ϵ is the unperturbed spectral deviation.

Proof. The unperturbed fractal exhibits discrete harmonics at frequencies $f_k = kf_0$ with amplitudes decaying as $|c_k| \propto k^{-(D-1)}$ [24]. The angular perturbation induces phase randomization:

$$\tilde{c}_k = c_k \cdot \exp(ik\Delta\theta) \quad (25)$$

For Gaussian-distributed $\Delta\theta$, the expected power spectrum becomes:

$$\mathbb{E}[|\tilde{c}_k|^2] = |c_k|^2 \cdot \mathbb{E}[\exp(2ik\Delta\theta)] \quad (26)$$

$$= |c_k|^2 \cdot \exp(-k^2\sigma_t^2) \quad (27)$$

This exponential suppression of high-frequency components approaches the natural image spectrum as σ_t increases, ensuring spectral indistinguishability.

D. Poisoning Efficiency Optimization

We derive the fundamental efficiency advantage of FTDBA in terms of required poisoning samples.

Theorem 4 (Sample Complexity Comparison). To achieve attack success rate $ASR \geq \tau$, the required number of poisoned samples satisfies:

$$\frac{N_{FTDBA}}{N_{DBA}} = \mathcal{O}(n^{-\alpha(1-1/D)}) \quad (28)$$

where n is the decomposition granularity and α is the strength decay exponent. The efficiency ratio in Eq. (28) quantifies our method's advantage, showing exponential reduction in required poisoning samples as decomposition granularity n increases.

Proof. The attack success rate follows a sigmoid relationship with the accumulated trigger strength:

$$ASR = \sigma \left(\sum_{i=1}^k S_i \cdot \frac{N_i}{C_i} \right)$$

where $\sigma(\cdot)$ is the sigmoid function, N_i is the number of poisoned samples, and C_i is the total dataset size for client i .

For traditional DBA with strength $S_i^{DBA} = S_{global}/n^\alpha$:

$$N_{DBA} = \frac{\sigma^{-1}(\tau) \cdot C}{S_{global}} \cdot n^\alpha$$

For FTDBA with enhanced strength $S_i^{FTDBA} = S_{global} \cdot n^{-\alpha/D} \cdot \psi(D)$:

$$N_{FTDBA} = \frac{\sigma^{-1}(\tau) \cdot C}{S_{global} \cdot \psi(D)} \cdot n^{\alpha/D}$$

Taking the ratio and noting that $\psi(D) \approx 1$ for $D \in [1.2, 1.4]$:

$$\frac{N_{FTDBA}}{N_{DBA}} = n^{\alpha(1/D-1)} = n^{-\alpha(1-1/D)} \quad (29)$$

Since $D > 1$, we have $N_{FTDBA} < N_{DBA}$ with the gap widening as n increases. For Koch curves with $D = 1.26$ and $\alpha = 0.8$, this yields approximately 62.4% reduction in required samples.

E. Convergence Analysis in Federated Learning

A critical concern is whether FTDBA disrupts the convergence properties of federated learning.

Theorem 5 (Convergence Preservation). Under FTDBA with perturbation bound $\|\delta_i\|_\infty \leq \epsilon$, the federated learning algorithm maintains convergence with rate:

$$\mathbb{E}[\mathcal{L}(w_t) - \mathcal{L}^*] \leq \frac{C_1}{t} + C_2\epsilon^2$$

where C_1, C_2 are constants depending on the learning rate and data heterogeneity.

Proof. The convergence analysis follows from the standard federated learning convergence proof with additional perturbation terms. Let g_i^t be the gradient at client i in round t . Under FTDBA:

$$\tilde{g}_i^t = \nabla \mathcal{L}(w_t; D_i^{clean}) + \lambda \nabla \mathcal{L}(w_t; D_i^{poison}) \quad (30)$$

$$= g_i^t + \lambda \nabla \mathcal{L}(w_t; \{x_j + \delta_i, y_{target}\}) \quad (31)$$

The perturbation term is bounded by:

$$\|\lambda \nabla \mathcal{L}(w_t; \{x_j + \delta_i, y_{target}\}) - \lambda \nabla \mathcal{L}(w_t; \{x_j, y_{target}\})\|_2 \leq L\lambda\epsilon$$

where L is the Lipschitz constant of the loss function. Since the poisoning ratio is small ($\lambda \ll 1$) and $\epsilon = 0.05$, the perturbation effect diminishes as $O(\epsilon^2)$, preserving convergence.

Theorem 6 (Communication Complexity). FTDBA maintains the same communication complexity $\mathcal{O}(K \cdot d \cdot T)$ as standard federated learning, where K is the number of clients, d is the model dimension, and T is the number of rounds.

Proof. The fractal trigger generation and perturbation are performed locally at each malicious client. Only the standard model updates are communicated to the server, requiring no additional communication overhead. The trigger coordination can be achieved through pre-shared fractal parameters, adding only $\mathcal{O}(1)$ initial setup cost.

F. Information-Theoretic Stealth Guarantee

Finally, we establish the stealth properties from an information-theoretic perspective.

Theorem 7 (KL Divergence Bound). Under the three-stage dynamic perturbation mechanism, the KL divergence between triggered and clean data distributions satisfies:

$$D_{KL}(P_{trigger} \| P_{data}) \leq \frac{L_\delta^2 \|\delta\|_\infty^2}{2} + \mathcal{O}(\sigma_t^2) \quad (32)$$

where L_δ is the Lipschitz constant of the loss gradient with respect to input perturbations. The bound in Eq. (32) provides information-theoretic stealth guarantee, ensuring undetectability under statistical analysis.

Proof. Following the analysis in [25], the KL divergence can be bounded using gradient similarity:

$$D_{KL} \leq \frac{1}{2} \mathbb{E} [\|\nabla_x \ell(x + \delta, y_{target}) - \nabla_x \ell(x, y_{true})\|_2^2]$$

TABLE II
FTDBA PARAMETER CONFIGURATION

Parameter	Value	Optimization Basis
D	1.26	Koch curve
α	0.8	$R^2 = 0.98$ (power law)
η	0.1π	$\Delta\theta \leq 6^\circ$
λ	10	ASR saturation
$T_{1,2}$	$0.3T/0.7T$	Cosine annealing

By the Lipschitz property and the constraint $\|\delta\|_\infty \leq 0.05$:

$$D_{KL} \leq \frac{L_\delta^2}{2} \cdot \|\delta\|_2^2 \leq \frac{L_\delta^2 d}{2} \cdot \|\delta\|_\infty^2$$

where d is the input dimension. The dynamic perturbation contributes an additional $\mathcal{O}(\sigma_t^2)$ term due to the randomization effect, which vanishes as $t \rightarrow T$ in the final stage. With $\|\delta\|_\infty = 0.05$ and typical values of $L_\delta \approx 1$, this yields $D_{KL} \leq 0.025$, consistent with our experimental observations.

These theoretical results collectively demonstrate that FTDBA achieves a fundamental improvement in the efficiency-stealth trade-off by leveraging the mathematical properties of fractal geometry and adaptive perturbation strategies, while preserving the convergence and communication properties of federated learning.

G. Experimental Setup and Environment

Experiments were conducted on a compute cluster with 4×NVIDIA A100 32GB GPUs and dual Intel Xeon Gold 6348 CPUs. To comprehensively evaluate performance, we used CIFAR-10 and ImageNet as benchmarks, representing medium and large-scale learning scenarios. The federated system simulates training with 100 clients. For CIFAR-10 experiments, we use $\rho = 10\%$ (10 malicious clients), while for ImageNet experiments, we use $\rho = 15\%$ (15 malicious clients) to account for the increased complexity of the dataset. The choice of higher ρ for ImageNet is justified by the need to maintain sufficient attack strength in the more challenging classification scenario. The model architecture is ResNet-18, optimized using SGD (initial learning rate 0.01, momentum 0.9).

Three categories of distributed backdoor baselines are compared: traditional spatial decomposition (DBA), latent feature perturbation (LFP), and natural-style triggers (NST). Evaluation includes:

- 1) **Attack effectiveness:** ASR and minimum poisoned sample count required
- 2) **Stealth:** KL divergence, SSIM, and PSNR metrics
- 3) **Defensibility:** Detection rate under 5 state-of-the-art defenses

Table II details key FTDBA parameters, optimized via grid search.

All results are averaged over 5 independent runs. Significance is tested via two-tailed t -test at 95% confidence.

H. Effectiveness Comparison

FTDBA shows substantial improvements in poisoning efficiency.

On CIFAR-10 with $\rho = 10\%$, FTDBA reaches 92.3% ASR using only 1,250 poisoned samples (95%CI : 91.7%–92.9%), outperforming NST by 5.5 percentage points. On ImageNet with $\rho = 15\%$, FTDBA achieves 89.7% ASR with 8,400 samples, maintaining effectiveness across different dataset complexities.

When targeting 90% ASR, only 1,120 samples are needed—just 62.4% of the DBA requirement. On ImageNet ($\rho = 15$), FTDBA reaches 89.7% ASR with 8,400 samples, whereas DBA needs 13,200.

This efficiency stems from the fractal dimension’s strength compensation. According to our theoretical analysis (Eq. (21)), the strength preservation factor $\psi(D) \approx 0.95$ for Koch curves, while the Hausdorff measure ratio maintains sub-trigger effectiveness. The sample complexity advantage predicted by Eq. (28) is empirically validated, showing $\gamma = n^{0.22} = 2.3$ improvement over traditional methods at decomposition granularity $n = 16$, sub-trigger strength is $2.3\times$ that of traditional methods ($\gamma = n^{\alpha(1-1/D)} = 16^{0.22}$), as shown in Table III. At decomposition granularity $n = 16$, sub-trigger strength is $2.3\times$ that of traditional methods ($\gamma = n^{\alpha(1-1/D)} = 16^{0.22}$), as shown in Table III.

TABLE III
ATTACK EFFECTIVENESS ON CIFAR-10 ($\rho = 10\%$, $n = 16$)

Method	N	ASR (%)	95% CI	Ratio
DBA	1795	78.5	[77.2, 79.8]	1.60×
LFP	1520	85.2	[84.1, 86.3]	1.36×
NST	1430	86.8	[85.9, 87.7]	1.28×
FTDBA	1120	92.3	[91.7, 92.9]	1.00×

Efficiency ratio = $N_{\text{method}}/N_{\text{FTDBA}}$.

I. Stealth Evaluation

Quantitative results show FTDBA outperforms others in both perceptual and statistical stealth. Table IV shows FTDBA’s KL divergence is only 0.018 (+/-0.002), a 41.2% reduction vs. DBA. SSIM reaches 0.983, and PSNR improves to 44.6 dB. Gradient analysis shows 36.7% of DBA’s variation, explaining the KL drop. These results validate our theoretical bound from Eq. (32), where the measured KL divergence of 0.018 falls well within the predicted upper bound of 0.025, demonstrating the effectiveness of our dynamic perturbation mechanism (Eqs. (5)-(6)).

J. Defense Robustness Evaluation

Against five SOTA defenses, FTDBA shows strong evasion. As shown in Table III, under Spectral Anomaly Detection, FTDBA achieves only 12.3% detection rate, 22.8 points lower than DBA. Its 18.7% rate is also significantly below NST’s 27.9%.

TABLE IV
STEALTH METRIC COMPARISON

Method	KL Div.	SSIM	PSNR (dB)
DBA	0.0306	0.962	38.2
LFP	0.0251	0.978	41.5
NST	0.0213	0.981	42.8
FTDBA	0.0180	0.983	44.6

TABLE V
DETECTION RATES UNDER SOTA DEFENSES (% , 95% CI)

Defense Method	DBA	LFP	NST	FTDBA
Spectral Anomaly	35.1±2.1	28.3±1.8	24.6±1.5	12.3±1.2
Neural Cleanse	41.7±2.3	32.5±2.0	29.1±1.7	14.9±1.4
ABS	38.4±2.2	31.2±1.9	27.8±1.6	13.5±1.3
FL-Defender	33.9±2.0	26.4±1.7	22.1±1.4	10.2±1.1
FoolsGold	29.5±1.8	23.8±1.6	19.3±1.3	8.7±0.9

Results averaged over 10 independent runs with different random seeds.

In gradient-based defenses, the malicious update norm $\|\Delta w_i^{\text{mal}} - \Delta w_i^{\text{clean}}\|_2 = 0.07$ is well below the 0.15 threshold, thanks to the final-stage micro-perturbation (when $\Delta\theta_i \leq 6^\circ$).

K. Ablation and Parameter Analysis

We systematically validate the necessity of FTDBA’s key components and quantify parameter impact, using CIFAR-10 with $\rho = 10$ and $n = 16$, averaged over 5 trials.

1) *Impact of Fractal Dimension*: Fractal dimension D is key to balancing effectiveness and stealth. As shown in Table VI, increasing D from 1.0 to 1.26 improves ASR from 76.4% to 92.3% and boosts γ from 1.00 to 2.30. However, beyond $D = 1.26$, KL increases (e.g., $D = 1.38$ leads to 0.024, a 33.3% rise), and spectral detection increases due to more harmonics.

2) *Ablation on Perturbation Mechanism*: The three-stage perturbation is crucial for avoiding exposure. Table VII shows disabling early wide perturbation ($t \leq T_1$) raises DR to 41.2%. Removing late micro-perturbation ($t > T_2$) increases KL to 0.035. Fixed Gaussian reduces DR to 24.7% but triggers gradient anomalies.

The full three-stage strategy optimizes: initial noise raises spectral entropy from 3.1 to 5.2 bit/Hz; mid-stage balances ASR; final stage reduces gradient deviation by 42.7%.

3) *Parameter Sensitivity*: Table VIII shows gradient mask λ , poisoning size N , and dimension D sensitivities:

- $\lambda \in [5, 8]$ shows strong linear sensitivity; beyond 8, ASR saturates; above 15, DR > 20%
- N follows $\text{ASR} = 1 - e^{-0.0021N}$ ($R^2 = 0.98$); 1120 is the 90% target
- D optimal in $[1.2, 1.3]$; above 1.3, KL rises sharply (e.g., $D = 1.35 \Rightarrow KL = 0.022 \approx \varepsilon$)

V. LIMITATIONS AND DISCUSSION

While FTDBA demonstrates significant advantages in attack efficiency and stealth, our comprehensive evaluation reveals

TABLE VI
IMPACT OF FRACTAL DIMENSION (D)

D	ASR (%)	KL	Δ KL	DR (%)	γ
1.00	76.4	0.0306	–	35.1	1.00
1.15	87.6	0.0221	27.8%	24.3	1.92
1.26	92.3	0.0180	41.2%	12.3	2.30
1.38	94.1	0.0240	21.6%	18.5	2.65
1.50	93.7	0.0272	11.1%	22.1	2.82

TABLE VII
ABLATION STUDY OF PERTURBATION MECHANISM

Configuration	ASR (%)	KL	DR (%)	$ \nabla \ell _2$
Fractal only	95.1	0.0192	41.2	0.063
+ Fixed Gaussian	89.3	0.0225	24.7	0.085
+ Two-Stage	90.6	0.0201	18.9	0.074
Full FTDBA	92.3	0.0180	12.3	0.051

several important limitations and considerations that warrant careful discussion.

A. Parameter Sensitivity and Tuning Complexity

Multi-Parameter Optimization: FTDBA’s effectiveness depends on careful tuning of multiple interdependent parameters (D , λ , σ_{max} , σ_{min} , T_1 , T_2). Our sensitivity analysis reveals that suboptimal parameter choices can significantly degrade performance. For instance, a 0.1 deviation in fractal dimension D from the optimal 1.26 results in 15-20% ASR reduction, making the method less robust to parameter estimation errors compared to traditional attacks.

Dataset-Specific Adaptation: While our adaptive parameter selection algorithm (Algorithm 2) provides general guidelines, optimal parameters still require dataset-specific fine-tuning. Cross-dataset experiments show that parameters optimized for CIFAR-10 achieve only 78.4% effectiveness when directly applied to ImageNet, necessitating recalibration for each new domain.

Hyperparameter Brittleness: The three-stage perturbation mechanism exhibits sensitivity to timing parameters T_1 and T_2 . Deviations of $\pm 10\%$ from optimal transition points (0.3T and 0.7T) increase detection rates by 5-8%, suggesting limited tolerance for estimation errors in federated learning convergence patterns.

B. Defense Adaptability and Arms Race Dynamics

Fractal-Aware Defenses: Our current evaluation focuses on existing defense mechanisms not specifically designed for fractal patterns. Future defense systems could incorporate fractal dimension analysis, self-similarity detection, or spectral analysis tuned for Koch curve signatures. Preliminary analysis suggests that defenses monitoring Hausdorff dimension variations could potentially detect FTDBA with 40-50% accuracy, significantly higher than current 12.3% detection rate.

Temporal Pattern Recognition: The three-stage perturbation strategy creates detectable temporal signatures in gradient evolution. Advanced defenses employing time-series analysis

TABLE VIII
PARAMETER SENSITIVITY ANALYSIS

Parameter	Optimal	Sensitivity	Limits
$\lambda \in [1, 20]$	10	[5,8]	\uparrow ASR slope < 0.5% (if > 8) \uparrow DR > 20% (if > 15)
$N \in [500, 2000]$	1120	[800,1200]	\uparrow ASR slope < 0.1% \uparrow KL > 0.025
$D \in [1.0, 1.5]$	1.26	[1.2,1.3]	\uparrow ASR slope < 0.3% $\partial \text{KL} / \partial D = 0.015$

of client updates could potentially identify the characteristic perturbation decay patterns, especially the transition phases at T_1 and T_2 .

Statistical Learning Resistance: While FTDBA achieves KL divergence of 0.018, this value remains distinguishable from pure noise ($KL \approx 0.005$). Machine learning-based defenses trained on large datasets of triggered and clean samples could potentially learn subtle statistical signatures that current rule-based defenses miss.

C. Methodological Limitations

Limited Dataset Diversity: Our evaluation focuses primarily on image classification tasks with CIFAR-10 and ImageNet. The effectiveness of fractal triggers in other modalities (text, audio, sensor data) remains unexplored and may exhibit different effectiveness patterns due to varying semantic structures.

Defense Evaluation Scope: We evaluate against five established defense mechanisms, but the rapidly evolving landscape of federated learning security may include newer defenses not covered in our analysis. Additionally, our evaluation assumes static defense parameters rather than adaptive defense strategies that could evolve during the attack.

Simulation vs. Reality Gap: Our experiments use simulated federated environments rather than true distributed deployments. Real-world factors such as system heterogeneity, network partitions, and operational constraints may significantly impact attack effectiveness in ways not captured by our controlled experimental setup.

VI. CONCLUSION

This paper proposes FTDBA, a novel distributed backdoor attack method based on fractal geometry. By leveraging self-similar structures, FTDBA enhances the attack strength of sub-triggers, enabling high attack success rates with significantly fewer poisoned samples. Theoretical analysis demonstrates that the fractal dimension D effectively mitigates the strength attenuation inherent in traditional decomposition. To address the detectability of fractal patterns, we design a three-stage dynamic perturbation mechanism that substantially improves stealth and robustness against detection. Experiments on CIFAR-10 and ImageNet validate the advantages of FTDBA in poisoning efficiency, stealthiness, and resistance to defenses. Future work will explore adaptive optimization of fractal parameters and new defense strategies tailored against FTDBA. This study offers a new perspective for designing efficient and stealthy attacks in federated learning.

REFERENCES

- [1] B. McMahan, E. Moore, D. Ramage, S. Hampson, and B. A. y Arcas, "Communication-efficient learning of deep networks from decentralized data," in *Artificial intelligence and statistics*. PMLR, 2017, pp. 1273–1282.
- [2] E. Bagdasaryan, A. Veit, Y. Hua, D. Estrin, and V. Shmatikov, "How to backdoor federated learning," vol. 108, pp. 2938–2948, 26–28 Aug 2020. [Online]. Available: <https://proceedings.mlr.press/v108/bagdasaryan20a.html>
- [3] G. Baruch, M. Baruch, and Y. Goldberg, "A little is enough: Circumventing defenses for distributed learning," *Advances in Neural Information Processing Systems*, vol. 32, 2019.
- [4] C. Xie, K. Huang, P.-Y. Chen, and B. Li, "Dbas: Distributed backdoor attacks against federated learning," in *International conference on learning representations*, 2019.
- [5] Z. Sun, P. Kairouz, A. T. Suresh, and H. B. McMahan, "Can You Really Backdoor Federated Learning?" Dec. 2019, arXiv:1911.07963 [cs, stat]. [Online]. Available: <http://arxiv.org/abs/1911.07963>
- [6] J. Cannon, "The fractal geometry of nature. by benoit b. mandelbrot," *The American Mathematical Monthly*, vol. 91, no. 9, pp. 594–598, 1984.
- [7] Y. Liu, Y. Xie, and A. Srivastava, "Neural trojans," in *2017 IEEE International Conference on Computer Design (ICCD)*. IEEE, 2017, pp. 45–48.
- [8] I. J. Goodfellow, J. Shlens, and C. Szegedy, "Explaining and harnessing adversarial examples," *stat*, vol. 1050, p. 20, 2015.
- [9] C. Fung, C. J. M. Yoon, and I. Beschastnikh, "Mitigating Sybils in Federated Learning Poisoning," Jul. 2020, arXiv:1808.04866 [cs, stat]. [Online]. Available: <http://arxiv.org/abs/1808.04866>
- [10] N. Carlini and D. Wagner, "Towards evaluating the robustness of neural networks," in *2017 IEEE Symposium on Security and Privacy (SP)*, 2017, pp. 39–57.
- [11] T. Gu, K. Liu, B. Dolan-Gavitt, and S. Garg, "Badnets: Evaluating backdooring attacks on deep neural networks," *IEEE Access*, vol. 7, pp. 47 230–47 244, 2019.
- [12] X. Chen, C. Liu, B. Li, K. Lu, and D. Song, "Targeted backdoor attacks on deep learning systems using data poisoning," *arXiv preprint arXiv:1712.05526*, 2017.
- [13] B. Tran, J. Li, and A. Madry, "Spectral signatures in backdoor attacks," *Advances in neural information processing systems*, vol. 31, 2018.
- [14] Y. Li, Y. Li, B. Wu, L. Li, R. He, and S. Lyu, "Invisible backdoor attack with sample-specific triggers," in *Proceedings of the IEEE-CVF international conference on computer vision*, 2021, pp. 16 463–16 472.
- [15] J. Jia, Y. Liu, and N. Z. Gong, "Badencoder: Backdoor attacks to pre-trained encoders in self-supervised learning," 2021. [Online]. Available: <https://arxiv.org/abs/2108.00352>
- [16] P. Blanchard, E. M. El Mhamdi, R. Guerraoui, and J. Stainer, "Machine learning with adversaries: Byzantine tolerant gradient descent," *Advances in neural information processing systems*, vol. 30, 2017.
- [17] B. Wang, Y. Yao, S. Shan, H. Li, B. Viswanath, H. Zheng, and B. Y. Zhao, "Neural cleanse: Identifying and mitigating backdoor attacks in neural networks," in *2019 IEEE Symposium on Security and Privacy (SP)*. IEEE, 2019, pp. 707–723.
- [18] J. Tan, X. Chen, Z. Wang, and Y. Li, "On the spectral properties of backdoor attacks," *arXiv preprint arXiv:1811.00636*, 2018.
- [19] I. Loshchilov and F. Hutter, "Sgdr: Stochastic gradient descent with warm restarts," in *International Conference on Learning Representations (ICLR)*, 2017.
- [20] Z. Wang, A. C. Bovik, H. R. Sheikh, and E. P. Simoncelli, "Image quality assessment: from error visibility to structural similarity," *IEEE transactions on image processing*, vol. 13, no. 4, pp. 600–612, 2004.
- [21] J. E. Hutchinson, "Fractals and self-similarity," *Indiana University Mathematics Journal*, vol. 30, no. 5, pp. 713–747, 1981.
- [22] K. Falconer, *Fractal geometry: mathematical foundations and applications*, 3rd ed. John Wiley & Sons, 2014.
- [23] B. B. Mandelbrot, *The Fractal Geometry of Nature*. W. H. Freeman, 1982.
- [24] M. V. Berry, "Diffractals," *Journal of Physics A: Mathematical and General*, vol. 12, no. 6, pp. 781–797, 1979.
- [25] N. Carlini and D. Wagner, "Towards evaluating the robustness of neural networks," in *2017 IEEE Symposium on Security and Privacy (SP)*. IEEE, 2017, pp. 39–57.